Progress In Electromagnetics Research, Vol. 112, 23–40, 2011

A NEW LOW SAR ANTENNA STRUCTURE FOR WIRELESS HANDSET APPLICATIONS

A. H. Kusuma, A.-F. Sheta, I. Elshafiey, Z. Siddiqui M. A. Alkanhal, S. Aldosari, and S. A. Alshebeili

Electrical Engineering Department and Prince Sultan Advanced Technologies Research Institute (PSATRI/STC-Chair)
King Saud University, P. O. Box 800, Riyadh 11421, Saudi Arabia

S. F. Mahmoud

Electrical Engineering Department
Kuwait University, P. O. Box 5969, Safat 13060, Kuwait

Abstract—This paper proposes a new mobile handset antenna structure to reduce the value of the specific absorption rate (SAR). The antenna is based on the PIFA structure and operates at dual-bands of 0.9 GHz and 1.8 GHz. The chassis current is reduced using a metallic shim-layer inserted between the patch and chassis. This shim-layer is connected to the handset chassis through posts whose number and positions are determined using optimization techniques. Sidewalls are attached to increase the gain of the antenna and reduce the radiation towards human head. Simulations in the cheek mode show that the SAR reduction factor (SRF) of the proposed structure averaged over 10-g is more than 75% at 0.9 GHz and 46% at 1.8 GHz. The SRF values obtained using simulations and measurements are found to be better than 51% and 76% at 0.9 GHz and 1.8 GHz, respectively.

1. INTRODUCTION

Mobile cellular telecommunications services are becoming widely spread around the world. Mobile handsets are often used in the vicinity of the human head. The continuous growth of wireless mobile services has forced the worldwide mobile handset manufacturers to consider the mutual interactions between the mobile terminals and human

Received 18 October 2010, Accepted 8 December 2010, Scheduled 24 December 2010
Corresponding author: Ibrahim Elshafiey (ishafiey@ksu.edu.sa).

body. On the one hand, part of the electromagnetic wave radiated by the antenna is absorbed by the human head. On the other hand, some mobile handset antenna characteristics, such as radiation pattern, radiation efficiency, bandwidth, and return loss, are altered due to the proximity of the human head. The mutual effects between the human head and the antenna have been investigated by many researchers [1–5]. The Specific Absorption Rate (SAR) is a defined parameter for evaluating the power absorption in human tissue. To protect the users from hazardous RF exposure, safety guidelines or limits of SAR have been made by Federal Communication Commission (FCC). According to IEEE, SAR is the time derivative of the incremental energy absorbed by (dissipated in) an incremental mass contained in a volume element of given density (ρ) [6]. The SAR limit is set at 2 W/kg over any 10 g of tissue according to IEEE C95.1:2005 [6]. This limit is comparable to the limit specified by the International Commission on Non-Ionizing Radiation Protection guidelines [7].

Planar Inverted F-Antenna (PIFA) is considered as one of the most appropriate antenna structures for mobile handset application due to many advantages including: low profile, simple structure, and reasonable antenna performance [8, 9]. PIFA structure is also attractive for designing multi-band antennas. These antennas are becoming essential for modern wireless communication systems [10, 11]. There are many methods proposed to PIFA structure to reduce SAR levels. The simplest method to significantly reduce SAR values depends on increasing the distance between the human head and the mobile handset antenna [12, 13]. This can be achieved by the application of back mounted antenna for mobile handset or by profiling the handset [14]. Other researchers try to reduce the radiation to human head by attaching a particular material to the antenna or mobile handset. Ferrite material has been an attractive material in reducing the SAR values [15, 16]. The effect of ferrite sheet attachment to mobile handset was also investigated by Wang et al. in 1999 [17]. The experiment is done using portable phone with a monopole antenna. The current from monopole antenna flows on all surfaces of the box. The ferrite sheet is used to suppress the current flowing in the handset box resulting in a significant reduction of the SAR without altering the antenna performance. The same technique for reducing the SAR values has recently been studied by Islam et al. in 2009 [18]. It is found that the ferrite attachment reduces the SAR values, due to the suppression of currents flowing on the front side of the mobile handset. Resistive sheet has also been investigated as a way to reduce SAR values by reducing the radiation toward the human head [19]. In 2006, Chan et al. investigated the effect of a sidewall attachment to the patch

antenna ground plane on SAR values [20]. It is found that the sidewall can noticeably reduce the SAR values.

In this paper, a new structure for reducing SAR values is investigated. The study is based on simulations performed under SEMCAD-X environment [21], and experimental measurements of SAR values achieved using DASY5 system [22, 23]. Since the electrical properties of the human head is frequency dependent, the dispersive model of the human head is incorporated in order to accurately predict the antenna behavior in the vicinity of the human head. The proposed antenna structure is presented in the following section, followed by the dispersion model calculations in Section 3. Simulation and experimental results along with discussions are presented in Section 4. Concluding remarks are presented in Section 5.

2. ANTENNA STRUCTURE

The proposed antenna is a PIFA with a modified ground structure designed to reduce the SAR values. In order to investigate the effect of the modified structure, two dual band antennas are designed. The first structure is the basic PIFA as shown in Figures 1(a) and 1(c), while the second antenna is the proposed PIFA with the modified ground structure, shown in Figures 1(b) and 1(d). The patch configuration of both antennas is kept the same. However, the first antenna is designed using a flat ground structure while the second one is designed with a new ground structure. Both antennas are designed to operate at 0.9 GHz and 1.8 GHz. The patch is placed 10 mm above the chassis. The total dimension of the patch is 25 mm $\times$ 26.5 mm and the dimension of the chassis is 40 mm $\times$ 80 mm. Coaxial probe is used to feed the antenna. The shorting pin of 2 mm diameter is located 1 mm far from the coaxial probe.

Figures 1(b) and 1(d) show the geometry of the antenna with the proposed ground structure. An additional thin metallic shim-layer is inserted between the patch and the chassis and placed 3 mm from the chassis as shown in Figure 1(d). This layer behaves as a new ground of the PIFA. Five conducting posts are used to connect the chassis and the intermediate shim-layer. The number and positions of the posts are determined using the optimization tool in SEMCAD-X, which is described in [24]. A total of five posts are implemented, where four posts are placed at the corners, while the fifth one is located at its center. In addition to the shim-layer, three conducting sidewalls are attached at the free sides of the antenna as shown in Figure 1(b), where the height of the sidewalls is 15 mm.

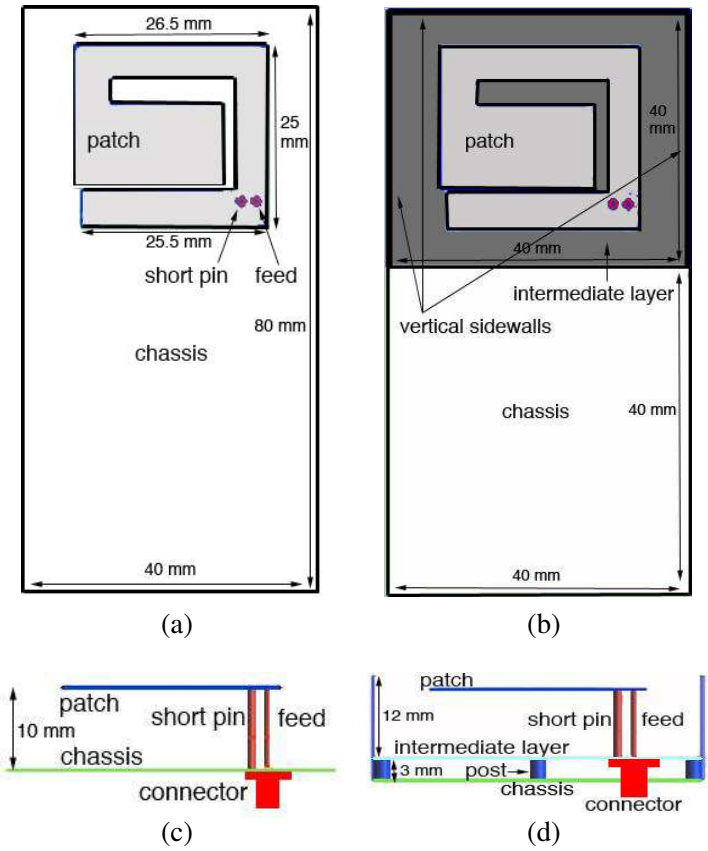

Figure 1. Antenna structure. (a) Top view of basic antenna structure. (b) Top view of antenna with the proposed ground structure. (c) Side view of basic antenna structure. (d) Side view of antenna with the proposed ground structure.

3. DISPERSIVE MODEL

SEMCAD-X simulation tool enables the user to calculate SAR values caused by the antenna radiation. SEMCAD-X is based on the FDTD method and is specialized in SAR computation. The human tissue parameters are frequency dependent. Therefore, dispersive material model should be considered to simulate the human head phantom. The relative permittivity of the human head decreases as the frequency increases and the electric conductivity increases as the frequency increases. The relative permittivity and electric conductivity of the

human head tissues is achieved using Lorentz model [21], which is accurate in simulating dispersive materials.

The dispersive material properties are achieved, using the dispersive material optimizer in SEMCAD-X. In this dispersive material optimization process, IEEE standard 1528 [25] for dielectric properties of human head is used as the reference to get the dispersion equation. Figure 2 shows the dispersive material properties used in the simulation. The error between the dielectric properties of human head in the IEEE standard 1528 and simulation is found to be approximately 3%.

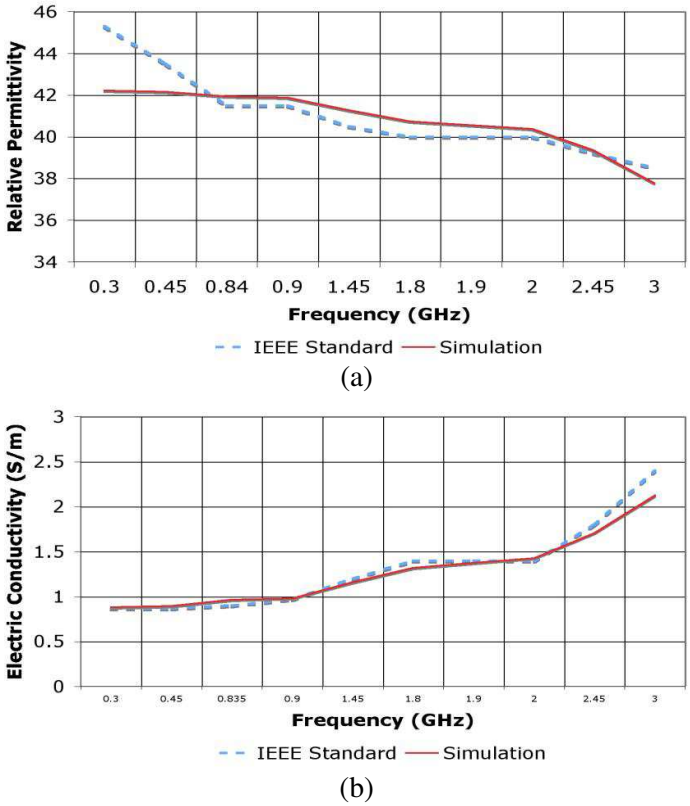

Figure 2. Dielectric properties of the human head model showing (a) relative permittivity and (b) electric conductivity.

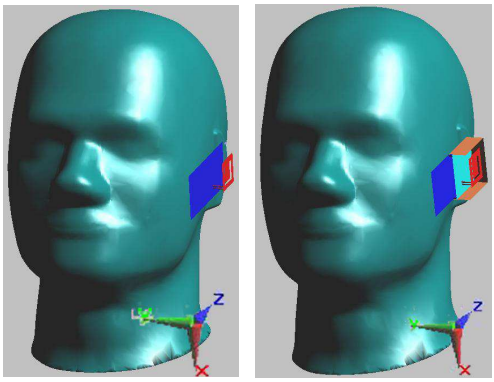

(a) (b)

Figure 3. Cheek mode. (a) Basic antenna structure. (b) Antenna with the proposed ground structure.

4. RESULTS AND DISCUSSIONS

The two designed antennas are simulated in cheek mode to investigate the effect of the proposed structure to the antenna performance in the vicinity of human head. In the cheek mode, the chassis of the antenna fully touches the cheek of the head model. The antenna-head position in this mode is shown in Figure 3.

4.1. Return Loss Measurements

The simulated and measured return losses of the basic antenna structure are shown in Figure 4. The measurements are performed by ANRITSU network analyzer 37369C. Simulating liquids of the human brain are used to investigate the human effect on the antenna return loss. The results show that the resonant frequencies of the basic antenna structure without human head model are 942 MHz for the first band, and 1913 MHz for the second band. The 6 dB bandwidths in free space of this antenna are 36 MHz for the first band and 180 MHz for the second band. When the basic antenna structure is placed in the cheek mode, the resonant frequencies become 920 MHz for the first band and 1896 MHz for the second band. The bandwidth of the first band and second band is increased to 43 MHz and 211 MHz, respectively. The figure clearly shows that the human head has a strong influence on the basic antenna structure.

Figure 5 shows the simulated and measured return loss of the antenna with the proposed ground structure. The resonant frequencies of the antenna with the proposed ground structure for the first

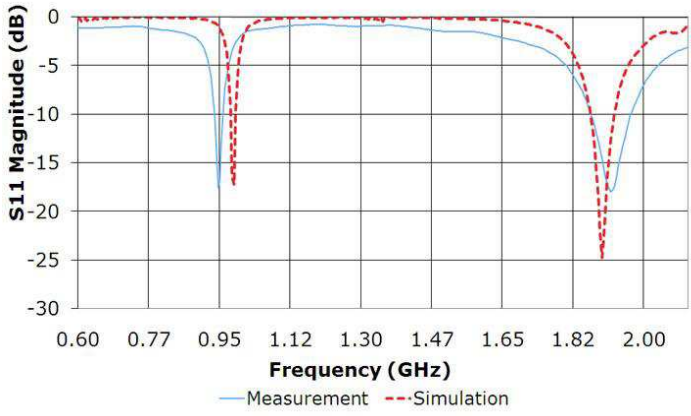

(a)

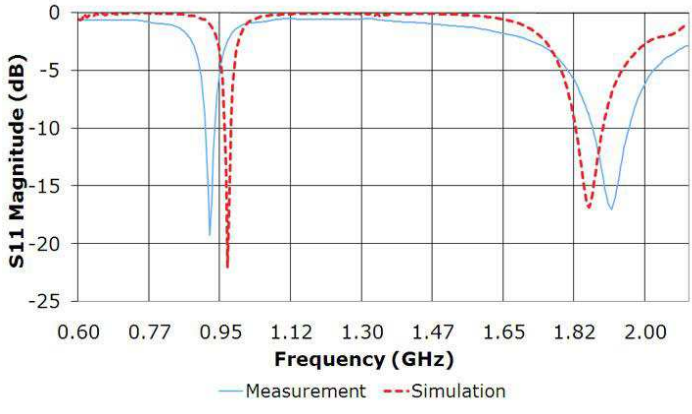

(b)

Figure 4. Simulated and measured return loss of basic antenna structure: (a) without human head, and (b) in the presence of human head.

and second bands without human head model are 902.5 MHz and 1703 MHz, respectively. The 6 dB bandwidths for the first and second bands are 22 MHz and 92 MHz, respectively. The resonant frequencies for the first and second bands in the vicinity of human head are 902.5 MHz and 1707 MHz, respectively. The bandwidths of the first and second bands are 25 MHz and 92 MHz, respectively. It is clear that the resonant frequencies and bandwidths are almost unchanged. Therefore, the proposed structure significantly decreases the influence of the human head to the antenna. It is worth noting that adding intermediate metallic layer and sidewalls to the basic antenna structure

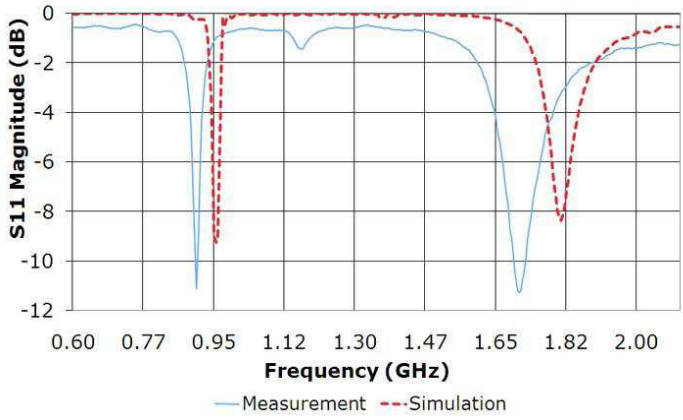

(a)

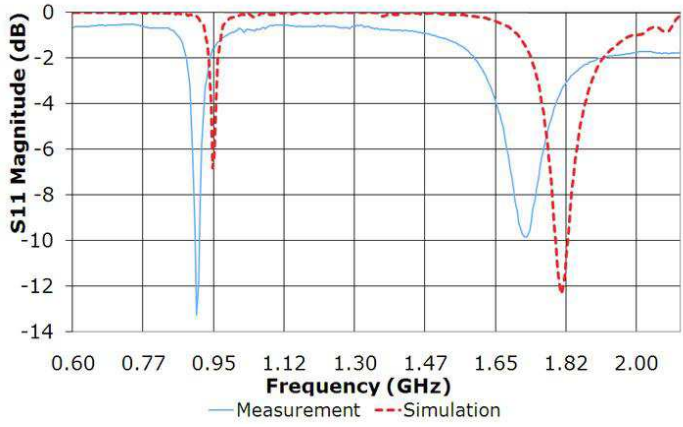

(b)

Figure 5. Simulated and measured return loss of antenna with the proposed ground structure: (a) without human head, and (b) in the presence of human head.

greatly decreases the resonant frequency and bandwidth of the antenna (from 920 to 902.5 MHz and from 1896 to 1707 MHz in the vicinity of the head).

4.2. Current Distribution

It is known that the chassis can be considered as a part of resonating element that contributes to the radiation to human head. Therefore, the intermediate layer is introduced to the basic antenna structure to reduce the current flowing on the chassis. Figure 6 shows the

current distributions of the basic antenna structure and antenna with the proposed ground structure. It is clearly shown in Figure 6 that the proposed structure greatly reduces the current flowing on the chassis.

4.3. Simulated Gain, SAR and Radiation Efficiency Results

Table 1 summarizes the simulation results of the basic antenna structure and antenna with the proposed ground structure. The gain and radiation efficiency of both antennas are tabulated in the absence of the human head and in its vicinity. A study of these numbers reveals that the new ground structure minimizes the effect of the human head to the radiation efficiency and gain. Namely, in the vicinity of human head, the radiation efficiency and gain of the basic antenna structure is noticeably decreased because of the power absorbed by human head. For example the gain at 900 MHz is decreased from +1.75 to −1.08 dBi due to the human head. On the other hand, the radiation efficiency and gain of the antenna with the proposed ground structure is only slightly decreased, indicating a lower absorbed power in the human head.

Table 2 compares the SAR simulation results for the basic antenna

Table 1. Simulated gain and radiation efficiency.

	Basic Antenna Structure		Antenna with the Proposed Shim-Layer	
	0.9 GHz	1.8 GHz	0.9 GHz	1.8 GHz
	Without Human Head Model			
Gain	1.75 dBi	1.83 dBi	0.91 dBi	1.76 dBi
Radiation Efficiency	94.78 %	97.78 %	78.58 %	94.35 %
	With Human Head Model			
Gain	−1.08 dBi	0.66 dBi	0.32 dBi	2.03 dBi
Radiation Efficiency	47.6%	61.03%	60.72%	68.41%

Table 2. SAR simulation results of cheek mode.

	Basic Antenna Structure		Antenna with the Proposed Shim-layer	
	0.9 GHz	1.8 GHz	0.9 GHz	1.8 GHz
Max 1-g Avg SAR	4.57 W/kg	1.49 W/kg	0.97 W/kg	0.87 W/kg
Max 10-g Avg SAR	2.69 W/kg	1.08 W/kg	0.67 W/kg	0.58 W/kg

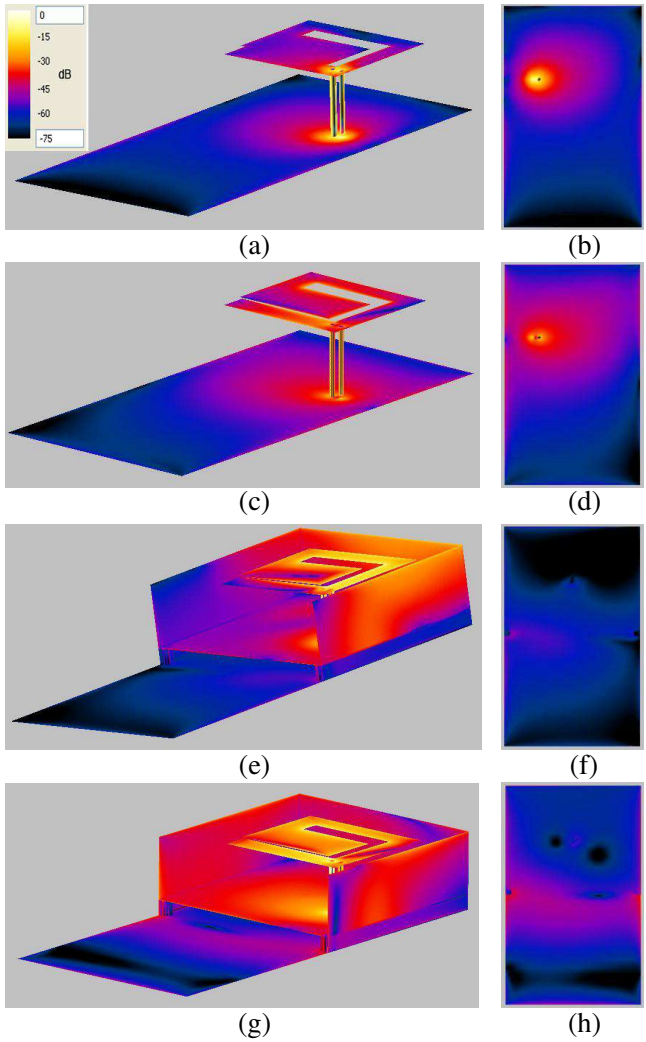

Figure 6. Current distribution. (a) Front side of basic antenna structure at 0.9 GHz. (b) Back side of basic antenna structure at 0.9 GHz. (c) Front side of basic antenna structure at 1.8 GHz. (d) Back side of basic antenna structure at 1.8 GHz. (e) Front side of antenna with the proposed ground structure at 0.9 GHz. (f) Back side of antenna with the proposed ground structure at 0.9 GHz. (g) Front side of antenna with the proposed ground structure at 1.8 GHz. (h) Back side of antenna with the proposed ground structure at 1.8 GHz.

and the antenna with the proposed ground structure in the cheek mode. The delivered power in this simulation is 0.5 W continuous signal. It is clearly shown that there is a great reduction in averaged SAR values at both bands for the proposed antenna. The maximum 1 g averaged SAR of the basic antenna structure and antenna with the proposed ground structure are 4.57 W/kg and 0.97 W/kg at 0.9 GHz and 1.49 W/kg and 0.87 W/kg at 1.8 GHz, respectively. The maximum 10 g averaged SAR of the basic antenna structure and antenna with the proposed ground structure are 2.69 W/kg and 0.67 W/kg at 0.9 GHz and 1.08 W/kg and 0.58 W/kg at 1.8 GHz. At 900 MHz, the maximum averaged 1 g and 10 g SAR are decreased by 78.8% and 75.1% by the new ground structure. For the 1800 MHz band, the maximum averaged 1 g and 10 g SAR are decreased by 41.61% and 46.3%, respectively.

4.4. The Radiation Pattern

The simulated radiation pattern of the total field of basic PIFA and the proposed antenna structures are shown in Figures 7 and 8. Total field is considered, since the polarization purity is not a big concern in mobile application [26, 27]. In the simulation, the head is positioned in the positive Y-axis as shown in Figure 3. The X and Z axes correspond to the width and length of the PIFA, respectively. Figure 7 shows the radiation pattern in the X-Y plane. The head lies at $\varphi = 90^\circ$ of the X-Y plane. The figures plot the simulated radiation patterns at the two resonances of the antenna in free space and in the presence of human head. Good omnidirectional radiation in the X-Y plane is seen for the basic antenna structure at both resonance frequencies in free space.

The peak antenna gain of the basic antenna structure and antenna with the proposed ground structure in free space (in the X-Y plane) is 1.67 dBi and 0.77 dBi at 0.9 GHz and 1.81 dBi and 1.75 dBi at 1.8 GHz, respectively. These gain values are computed in the X-Y plane while, the overall antenna gain is indicated in Table 1.

In the presence of human head, the radiation patterns of both structures are affected due to energy absorption by human head. The peak antenna gain of the basic antenna structure and antenna with the proposed ground structure in the presence of human head is -1.15 dBi and 0.12 dBi at 0.9 GHz and -0.47 dBi and 1.33 dBi at 1.8 GHz. This shows that, effect of the human head to the basic antenna structure is greater than the antenna with the proposed ground structure. Another important observation here is that, relative to the basic antenna, the radiation towards the head (along Y) is much less affected by the human head for the proposed antenna. This means that the head absorbs considerably less power for the proposed antenna than is the case with the basic antenna.

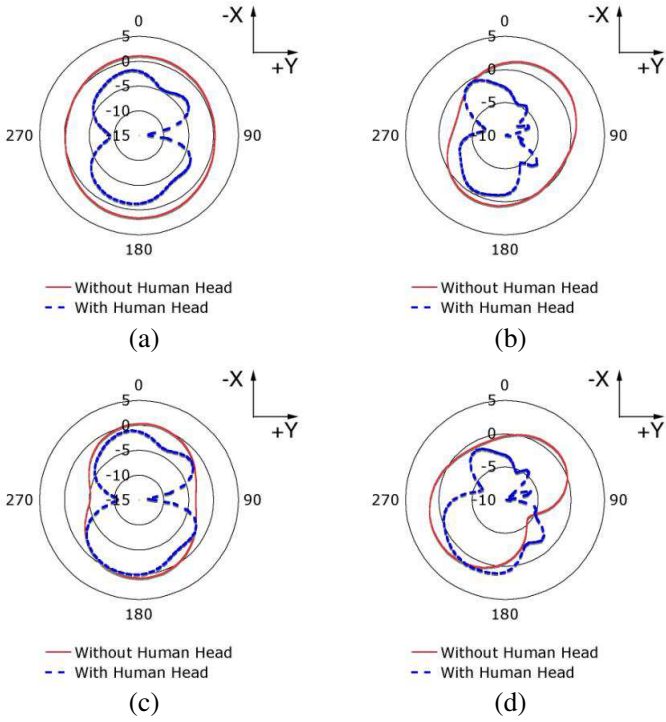

Figure 7. The xy-plane radiation patterns. (a) Basic antenna structure at 0.9 GHz. (b) Basic antenna structure at 1.8 GHz. (c) Antenna with the proposed ground structure at 0.9 GHz. (d) Antenna with the proposed ground structure at 1.8 GHz.

Figure 8 plots the simulated radiation pattern of the basic antenna structure and antenna with the proposed ground structure at both resonances in Y-Z plane. The human head lies at $\theta = 90°$ of Y-Z plane. The same conclusion drawn from Figure 7 can be drawn from Figure 8. An interesting observation is noticed in Figure 8(d), where little power is found to be absorbed and the radiation pattern is reshaped at 1.8 GHz. The gain is thus increased even above the case with no human head present as shown in Table 1.

4.5. Experimental Versus Simulation Results

Since the designed antennas are fed using coaxial probe, it is not practically possible to place the PIFA in cheek mode as shown in Figure 3. Therefore, the antennas are inclined by about 30° to give

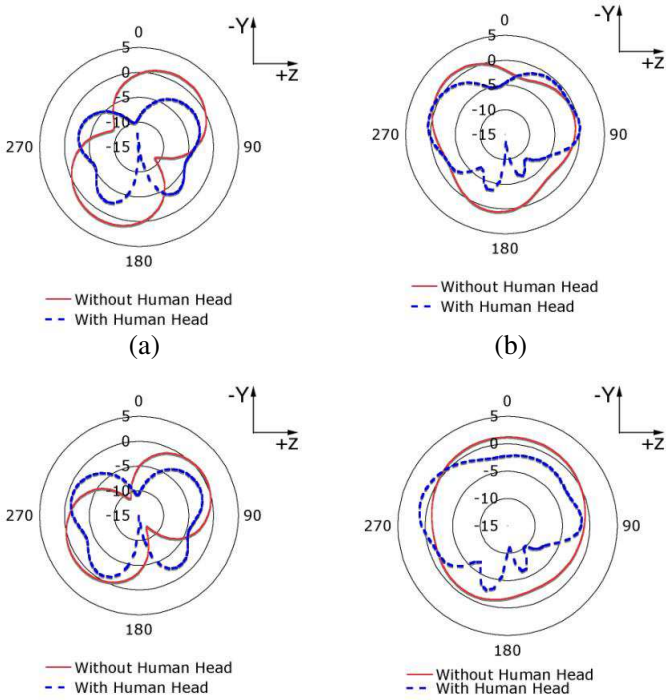

Figure 8. The yz-plane radiation patterns. (a) Basic antenna structure at 0.9 GHz. (b) Basic antenna structure at 1.8 GHz. (c) Antenna with the proposed ground structure at 0.9 GHz. (d) Antenna with the proposed ground structure at 1.8 GHz.

space to the connector as shown in Figure 9. Therefore, in this design, tilt mode seems appropriate for this practical characterization as shown in Figure 9. In this mode, only top and bottom part of the left side of the chassis touch the human head model.

The SAR measurement is performed using DASY 5 SAR measurement system. The system depends on a robot to position the SAR probe inside the human head phantom. The human head phantom is filled with a liquid with dielectric properties selected based on IEEE standard 1528, which are $\varepsilon_r = 41.5$ and $\sigma = 0.97\,\mathrm{S/m}$ for 0.9 GHz and $\varepsilon_r = 40$ and $\sigma = 1.4\,\mathrm{S/m}$ for 1.8 GHz. Measured and simulated SAR values are shown in Table 3 at the 900 and 1800 MHz bands for the basic antenna and the antenna with the proposed ground structure.

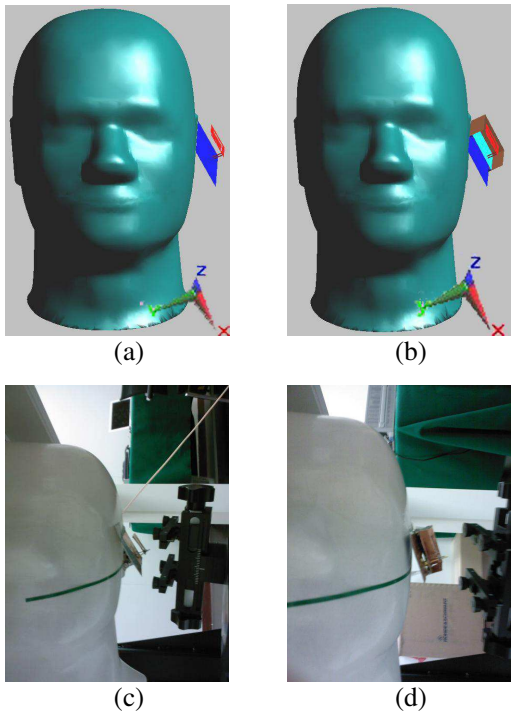

Figure 9. Antenna-head position. (a) Basic antenna structure position in tilt mode simulation. (b) Antenna with the proposed ground structure position in tilt mode simulation. (c) Basic antenna structure position in tilt mode measurement. (d) Antenna with the proposed ground structure position in tilt mode measurement.

The RF power delivered to the antenna is continuous and set at 0.5 W and the SAR values are given as the maximum 1 g and 10 g average. It is seen that for maximum 1 g averaged SAR, the measured SAR reduction factor (SRF) is 51.7% at 0.9 GHz and 76.7% at 1.8 GHz. For maximum 10 g averaged SAR, the measured SRF is 48.1% at 0.9 GHz and 74% at 1.8 GHz.

The measured SAR value for GSM applications should be divided by the crest factor of 8.3 to account for the small period of transmission corresponding to one out of 8 time slots (bursts). In this case the actual SAR values will be very small with respect to the allowed levels and less than most of the commercial mobile handset. As shown in the table, simulations and measurements are in very well agreement. It has to be noted that, the maximum SAR Reduction Factor (SRF)

Table 3. Simulated and measured SAR.

	Basic Antenna Structure		Antenna with the Proposed Shim-layer	
	0.9 GHz	1.8 GHz	0.9 GHz	1.8 GHz
Simulation results				
Max 1 g Avg SAR	2.3 W/kg	4 W/kg	1.03 W/kg	0.93 W/kg
Max 10 g Avg SAR	1.44 W/kg	2.09 W/kg	0.68 W/kg	0.54 W/kg
Measurement results				
Max 1 g Avg SAR	2.34 W/kg	3.86 W/kg	1.13 W/kg	0.9 W/kg
Max 10 g Avg SAR	1.31 W/kg	2.08 W/kg	0.68 W/kg	0.54 W/kg

recently reported in [18] using ferrite sheet is 57.75% at 1.8 GHz. The maximum SRF obtained by using R-card attachment at 0.9 GHz is 64% [19]. Therefore, the new ground structure proposed in this paper is a promising design for the new generations of low SAR mobile phones.

5. CONCLUSION

A low SAR mobile terminal antenna is designed, simulated, and fabricated. Three vertical sidewalls are attached to the antenna to increase the gain and reduce the radiation towards human head. An additional layer is also inserted between the patch and the chassis to reduce the current flowing on the chassis. The increased gain and reduced current flowing on the chassis decreases the radiation toward the human head and so reduces the SAR value. Simulations and measurements agree well and show that the SRF of the proposed structure is more than 48% at 0.9 GHz and more than 74% at 1.8 GHz. More effort is still needed in order to overcome some challenges such as the insufficient matching and bandwidth. Size reduction is valuable for modern communication terminals. Reducing the overall height will reduce the antenna bandwidth, and more investigation is currently directed towards reducing the size, while maintaining attractive SRF.

ACKNOWLEDGMENT

This research is funded by King Abdulaziz City for Science and Technology (KACST), Research Grant: MT-2-5.

REFERENCES

1. Christopoulou, M., S. Koulouridis, and K. S. Nikita, "Parametric study of power absorption patterns induced in adult and child head models by small helical antennas," *Progress In Electromagnetics Research*, Vol. 94, 49–67, 2009.
2. Hirata, A., K. Shirai, and O. Fujiwara, "On averaging mass of SAR correlating with temperature elevation due to a dipole antenna," *Progress In Electromagnetics Research*, Vol. 84, 221–237, 2008.
3. Mahmoud, K. R., M. El-Adawy, S. M. M. Ibrahem, R. Bansal, and S. H. Zainud-Deen, "Investigating the interaction between a human head and a smart handset for 4G mobile communication systems," *Progress In Electromagnetics Research C*, Vol. 2, 169–188, 2008.
4. Kouveliotis, N. K. and C. N. Capsalis, "Prediction of the SAR level induced in a dielectric sphere by a thin wire dipole antenna," *Progress In Electromagnetics Research*, Vol. 80, 321–336, 2008.
5. Ebrahimi-Ganjeh, M. A. and A. R. Attari, "Interaction of dual band helical and PIFA handset antennas with human head and hand," *Progress In Electromagnetics Research*, Vol. 77, 225–242, 2007.
6. IEEE Std C95.1-2005, "Safety levels with respect to human exposure to radio frequency electromagnetic fields, 3 kHz to 300 GHz," IEEE Standard, 2006.
7. ICNIRP Guidelines, "Guidelines for limiting exposure to time varying electric, magnetic and electromagnetic fields up to 300 GHz," *Health Phys.*, Vol. 74, No. 4, 1998.
8. Lazzi, G., J. Johnson, S. S. Pattnaik, and O. P. Gandhi, "Experimental study on compact, high-gain, low SAR single- and dual-band patch antenna for cellular telephones," *IEEE Antennas and Propagation Society International Symposium*, Vol. 1, 130–133, 1998.
9. Park, J. D., B. C. Kim, and H. D. Choi, "A low SAR design of folder type handset with dual antennas," *IEEE Antennas and Propagation Society International Symposium*, Vol. 2, 1005–1008, 2003.
10. Cheng, P.-C., C.-Y.-D. Sim, and C.-H. Lee, "Multi-band printed internal monopole antenna for mobile handset applications," *Journal of Electromagnetic Waves and Applications*, Vol. 23, No. 13, 1733–1744, 2009.
11. Zuo, S. L., Z. Y. Zhang, and Y. Z. Yin, "A planar meander monopole antenna for DVB-H/GSM/DCS mobile handsets,"

Journal of Electromagnetic Waves and Applications, Vol. 23, No. 17–18, 2331–2337, 2009.

12. Kivekas, O., J. Ollikainen, T. Lehtiniemi, and P. Vainikainen, "Bandwidth, SAR, and efficiency of internal mobile phone antennas," *IEEE Trans. Electromagn. Compat.*, Vol. 46, No. 1, 71–86, 2004.
13. Saraereh, O. A., M. Jayawardene, P. McEvoy, and J. C. Vardaxoglou, "Simulation and experimental SAR and efficiency study for a dual-band PIFA handset antenna (GSM 900/DCS 1800) at varied distance from a phantom head," *IEE Antenna Measurements and SAR*, 5–8, 2004.
14. Amos, S. V., M. S. Smith, and D. Kitchmer, "Modeling of handset antenna interactions with the user and SAR reduction techniques," *IEE National Conference on Antennas and Propagation*, 12–15, York, UK, 1999.
15. Kitra, M. I., C. J. Panagamuwa, P. McEvoy, J. C. Vardaxoglou, and J. R. James, "Low SAR ferrite handset antenna design," *IEEE International Workshop on Antenna Technology Small Antennas and Novel Metamaterials*, 144–147, 2006.
16. Kitra, M. I., C. J. Panagamuwa, P. McEvoy, J. C. Vardaxoglou, and J. R. James, "Low SAR ferrite handset antenna design," *IEEE Trans. Antennas Propag.*, Vol. 55, No. 4, 1155–1164, 2007.
17. Wang, J., O. Fujiwara, and T. Takagi, "Effect of ferrite sheet attachment to portable telephone in reducing electromagnetic absorption in human head," *IEEE International Symposium on Electromagnetic Compatibility*, Vol. 2, 822–825, 1999.
18. Islam, M. T., M. R. I. Faruque, and N. Misran, "Design analysis of ferrite sheet attachment for SAR reduction in human head," *Progress In Electromagnetic Research*, Vol. 98, 191–205, 2009.
19. Chou, H. H., H. T. Hsu, H. T. Chou, K. H. Liu, and F. Y. Kuo, "Reduction of peak SAR in human head for handset applications with resistive sheets (R-Cards)," *Progress In Electromagnetic Research*, Vol. 94, 281–296, 2009.
20. Chan, K. H., L. C. Fung, S. W. Leung, and Y. M. Siu, "Effect of internal patch antenna ground plane on SAR," *17th International Zurich Symposium on Electromagnetic Compatibility*, 513–516, 2006.
21. SEMCAD. *SEMCAD Manual*, Available online at http://www.semcad.com.
22. DASY5 Documentation, manufactured by SPEAG, http://www.speag.com.

23. Kusuma, A. H., "Antenna design for mobile terminals based on interactions with the human body," MS Thesis, King Saud University, Riyadh, Saudi Arabia, 2010.
24. Elshafiey, I., A.-F. Sheta, S. Aldosari, M. A. Alkanhal, and S. A. Alshebeili, "Multiobjective optimization for low SAR antenna design," *IEEE International Symposium on Signal Processing and Information Technology (ISSPIT)*, 213–218, 2009.
25. IEEE Std 1528-2003, "IEEE Recommended practice for determining the peak spatial-average specific absorption rate (SAR) in the human head from wireless communications devices: Measurement techniques," IEEE Standard, 2003.
26. Du, Z., K. Gong, and J. S. Fu, "A novel compact wide-band planar antenna for mobile handsets," *IEEE Trans. Antennas Propag.*, Vol. 54, No. 2, 613–619, 2006.
27. Ali, M., G. J. Hayes, H.-S. Hwang, and R. A. Sadler, "Design of a multiband internal antenna for third generation mobile phone handsets," *IEEE Trans. Antennas Propag.*, Vol. 51, No. 7, 1452–1461, 2003.